

METHODOLOGICAL NOTES PACS number: 42.30.Va

On the role of phantom sources in the theory of superlenses

L S Dolin

DOI: https://doi.org/10.3367/UFNe.2023.01.039317

Contents

Abstract. The effect of the appearance of 'phantom sources' in a theoretical model of an image formed by an ideal Veselago lens has been investigated by transformation optics (TO) methods. It is shown that this effect cannot be used to explain the mechanism of superlensing. A method is proposed for eliminating phantom sources in the construction of image models by TO methods. An expression is given for the electromagnetic field which forms an ideal image of a point radiation source when its distance from the front surface of the lens is equal to its thickness. An explanation is given as to why a rigorous model of the ideal image of a dipole source cannot be constructed if the distance between the source and the lens is shorter than its thickness.

Keywords: image, transformation optics, superlensing, ideal Veselago lens, phantom sources, dipole sources, ideal image model

1. Introduction

The Veselago lens [1], which is a plane layer of 'left-handed' matter (with a negative refractive index [2]), has become known as a superlens due to its ability to produce images with a spatial resolution that goes beyond the diffraction limit [3–22]. Cylindrical and spherical objects coated with 'left-handed' material may possess similar properties [23, 25–29]. It was shown that overcoming the diffraction limit becomes possible due to the amplification of the reactive near electromagnetic (EM) field of the observed radiation source by the left-handed medium [3]. To explain the 'superlensing' mechanism, advantage was also taken of the results of theoretical studies, according to which a left-matter lens with zero absorption should have the ability to generate 'phantom sources' — copies of the observed point source located at the points of its image [23, 27, 29]. The discovery of this effect led to the understanding of the basic need to take into account the absorption of radiation by the left-handed medium when analyzing the resolving power of superlenses [23, 24, 29].

In Refs [30, 31], attention was drawn to the following fact: in using transformation optics (TO) equations to calculate EM fields in a space with layers of left-handed matter, additional external currents similar to phantom sources may appear in Maxwell's equations. It was noted that, in the presence of such currents, the TO equations give the correct solution to the electrodynamic problem but not to the one posed: the resulting expression for the EM field describes not the image of a given source but the field of three extraneous sources.

This paper presents formulas for calculating phantom electric currents and charges and proposes a way to eliminate them when constructing a theoretical model of images formed by an ideal Veselago lens. The patterns of energy flow lines in the lens and the signs of phantom sources manifestation in these pictures are analyzed. A description is given of some image models constructed by TO methods using the operation of phantom source elimination.

2. Equations of transformation optics for studying lens properties

Let $\mathrm{Re}\,[\mathbf{E}^0(\mathbf{r})\exp(\mathrm{i}\omega t)]$, $\mathrm{Re}\,[\mathbf{H}^0(\mathbf{r})\exp(\mathrm{i}\omega t)]$ be the strengths of the monochromatic EM field generated in free space by electric currents and charges with volume density $\mathrm{Re}\,[\mathbf{j}^0(\mathbf{r})\exp(\mathrm{i}\omega t)]$, $\mathrm{Re}\,[\rho^0(\mathbf{r})\exp(\mathrm{i}\omega t)]$; $\mathbf{r} = \mathbf{r}_\perp + z\mathbf{z}_0$ is the radius vector of a point in space, $\mathbf{z}_0 = \nabla z$ is the unit vector of the z direction, and ω is the field frequency. By replacing the z variable with

$$z' = \xi(z) \tag{1}$$

and using the TO equations [32–36], we can construct a model of another EM field $\mathrm{Re}\,[\mathbf{E}(\mathbf{r})\exp(\mathrm{i}\omega t)]$, $\mathrm{Re}\,[\mathbf{H}(\mathbf{r})\exp(\mathrm{i}\omega t)]$,

L S Dolin
Federal Research Center A V Gaponov-Grekhov Institute of Applied Physics, Russian Academy of Sciences, ul. Ul'yanova 46, 603950 Nizhny Novgorod, Russian Federation
National Research Lobachevsky State University of Nizhny Novgorod, prosp. Gagarina 23, 603022 Nizhny Novgorod, Russian Federation
E-mail: lev.dolin@ipfran.ru, lev.dolin@mail.ru, Lev.Dolin@hydro.appl.sci-nnov.ru

Received 4 March 2022, revised 22 January 2023
Uspekhi Fizicheskikh Nauk **193** (8) 902 – 908 (2023)
Translated by E N Ragozin

produced by currents $\mathrm{Re}\,[\mathbf{j}(\mathbf{r})\exp(\mathrm{i}\omega t)]$ and charges $\mathrm{Re}\,[\rho(\mathbf{r})\exp(\mathrm{i}\omega t)]$ in a medium with diagonal permittivity and magnetic permeability tensors whose elements are expressed in terms of the function $\xi(z)$ as

$$\varepsilon_{xx}=\varepsilon_{yy}=\mu_{xx}=\mu_{yy}=\frac{\mathrm{d}\xi(z)}{\mathrm{d}z}\,,\qquad \varepsilon_{zz}=\mu_{zz}=\left[\frac{\mathrm{d}\xi(z)}{\mathrm{d}z}\right]^{-1}. \tag{2}$$

We represent the complex amplitudes of fields and currents as the sum of their transverse and longitudinal (with respect to the z-axis) components:

$$\begin{aligned}&\mathbf{E}^0(\mathbf{r}_\perp,z)=\mathbf{E}^0_\perp+E^0_z\mathbf{z}_0\,,\quad \mathbf{H}^0(\mathbf{r}_\perp,z)=\mathbf{H}^0_\perp+H^0_z\mathbf{z}_0\,,\\ &\mathbf{j}^0=\mathbf{j}^0_\perp+j^0_z\mathbf{z}_0\,,\\ &\mathbf{E}(\mathbf{r}_\perp,z)=\mathbf{E}_\perp+E_z\mathbf{z}_0\,,\quad \mathbf{H}(\mathbf{r}_\perp,z)=\mathbf{H}_\perp+H_z\mathbf{z}_0\,,\\ &\mathbf{j}=\mathbf{j}_\perp+j_z\mathbf{z}_0\,.\end{aligned} \tag{3}$$

Then, the relationship between the fields in free space and in a medium with constants (2) will be determined by the equations

$$\mathbf{E}_\perp(\mathbf{r}_\perp,z)=\mathbf{E}^0_\perp\big(\mathbf{r}_\perp,\xi(z)\big)\,,\quad E_z(\mathbf{r}_\perp,z)=\frac{\mathrm{d}\xi(z)}{\mathrm{d}z}\,E^0_z\big(\mathbf{r}_\perp,\xi(z)\big)\,, \tag{4}$$

$$\mathbf{H}_\perp(\mathbf{r}_\perp,z)=\mathbf{H}^0_\perp\big(\mathbf{r}_\perp,\xi(z)\big)\,,\quad H_z(\mathbf{r}_\perp,z)=\frac{\mathrm{d}\xi(z)}{\mathrm{d}z}\,H^0_z\big(\mathbf{r}_\perp,\xi(z)\big)\,,$$

$$\mathbf{j}_\perp(\mathbf{r}_\perp,z)=\frac{\mathrm{d}\xi(z)}{\mathrm{d}z}\,\mathbf{j}^0_\perp\big(\mathbf{r}_\perp,\xi(z)\big)\,,\quad j_z(\mathbf{r}_\perp,z)=j^0_z\big(\mathbf{r}_\perp,\xi(z)\big)\,, \tag{5}$$

$$\rho(\mathbf{r}_\perp,z)=\frac{\mathrm{d}\xi(z)}{\mathrm{d}z}\,\rho^0\big(\mathbf{r}_\perp,\xi(z)\big)\,,$$

which are applicable for an arbitrary unambiguous dependence $\xi(z)$. The relation between the time-averaged distributions of the Umov–Poynting vector in the indicated fields is described by the formulas

$$\begin{aligned}&\mathbf{S}=\frac{c}{8\pi}\,\mathrm{Re}\,\big[\mathbf{E}\mathbf{H}^*\big]=\mathbf{S}_\perp+S_z\mathbf{e}_z\,,\\ &\mathbf{S}^0=\frac{c}{8\pi}\,\mathrm{Re}\,\big[\mathbf{E}^0\mathbf{H}^{0*}\big]=\mathbf{S}^0_\perp+S^0_z\mathbf{z}_0\,,\\ &\mathbf{S}_\perp(\mathbf{r}_\perp,z)=\frac{\mathrm{d}\xi(z)}{\mathrm{d}z}\,\mathbf{S}^0_\perp\big(\mathbf{r}_\perp,\xi(z)\big)\,,\quad S_z(\mathbf{r}_\perp,z)=S^0_z\big(\mathbf{r}_\perp,\xi(z)\big)\,.\end{aligned} \tag{6}$$

By putting [37]

$$\xi(z)=\begin{cases}z\,, & z<0\,,\\ -z\,, & 0<z<z_0\,,\\ z-2z_0\,, & z>z_0\,,\end{cases} \tag{7}$$

we get the opportunity to use equations (4), (5) to study the properties of a plane 'superlens' of thickness z_0 of an isotropic material with constants $\varepsilon_{xx}=\varepsilon_{yy}=\varepsilon_{zz}=\mu_{xx}=\mu_{yy}=\mu_{zz}=-1$ and refractive index $n=-1$ (Fig. 1). In doing so, it is important to take into account that, according to equations (5), the sources of the fields $\mathbf{E}^0$, $\mathbf{H}^0$ and $\mathbf{E}$, $\mathbf{H}$ under certain conditions may differ, and equations (4) will not provide a solution to the problem posed. This difference arises due to the ambiguity of the function $z=z(\xi)$ for $-z_0<\xi<0$, which leads to the appearance of two additional sources in the space of variables $\mathbf{r}_\perp$, z if the coordinate of the source ξ_s in the space of variables $\mathbf{r}_\perp$, ξ satisfies the condition $-z_0<\xi_\mathrm{s}<0$.

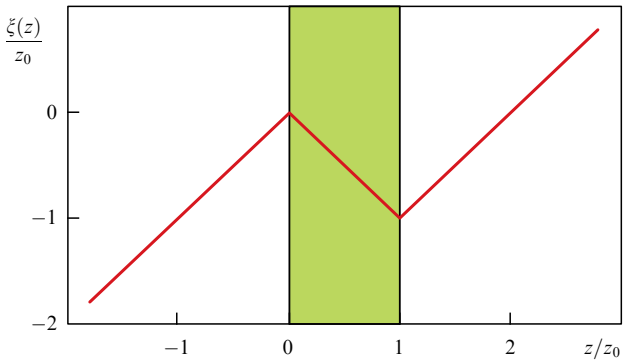

Figure 1. Type of transformation (7).

3. Focusing properties of a lens and conditions for the emergence of phantom sources

As suggested by formulas (4) and (7), when a lens is formed by a medium layer $0\leqslant z\leqslant z_0$ with a refractive index $n=-1$ and the field sources are in the region $z\leqslant -z_0$, i.e., are removed from the front surface of the lens at a distance greater than or equal to its thickness z_0, then the field behind the lens ($z>z_0$) has the form

$$\mathbf{E}(\mathbf{r}_\perp,z)=\mathbf{E}^0(\mathbf{r}_\perp,z-2z_0)\,,\quad \mathbf{H}(\mathbf{r}_\perp,z)=\mathbf{H}^0(\mathbf{r}_\perp,z-2z_0) \tag{8}$$

and, consequently, it is a copy of the EM field produced by the indicated sources in the absence of a lens in the free space region $-z_0<z<\infty$. The field on the rear side of the lens ($z=z_0$) reproduces the field distribution $\mathbf{E}^0$, $\mathbf{H}^0$ in the plane $z=-z_0$:

$$\mathbf{E}(\mathbf{r}_\perp,z_0)=\mathbf{E}^0(\mathbf{r}_\perp,-z_0)\,,\quad \mathbf{H}(\mathbf{r}_\perp,z_0)=\mathbf{H}^0(\mathbf{r}_\perp,-z_0)\,. \tag{9}$$

A plane wave remains plane after passing through the lens, and it focuses a spherical wave.

Figure 2 shows the energy flow lines calculated in the lens section by the plane $y=0$ when a spherical wave is produced by the electric current

$$\mathbf{j}^0=\mathbf{J}\delta(\mathbf{r}_\perp)\,\delta(z-z_\mathrm{s}) \tag{10}$$

under the conditions $\mathbf{J}=J\nabla y$, $z_\mathrm{s}\leqslant -z_0$. The calculations were performed using formulas (6) and the expression

$$\big[S^0_x\big]_{y=0}=\frac{Ax}{r^3}\,,\quad \big[S^0_z\big]_{y=0}=\frac{A(z-z_\mathrm{s})}{r^3}\,,$$

$$r=\sqrt{x^2+(z-z_\mathrm{s})^2}\,,\quad A=\frac{3P_\mathrm{s}}{4\pi}\,,$$

where P_s is the power of the source. As is clear from Fig. 2, at $z_\mathrm{s}<-z_0$, the lens forms a virtual image of a point source (10) shifted relative to the source towards the lens by its double thickness. As the source approaches the plane $z=-z_0$, the refraction points of different energy flow lines on the rear lens surface converge and merge at $z_\mathrm{s}=-z_0$ to form an ideal image of the source. The ideality of this image is also confirmed by formulas (9), according to which the field distribution on the rear side of the lens must correctly reproduce the field variations in the plane $z=-z_0$ on arbitrarily small spatial scales.

When the source is in the domain $-z_0<z<0$, coordinate transformation (7) along with the virtual layer of the 'left-handed' medium generates additional radiation sources

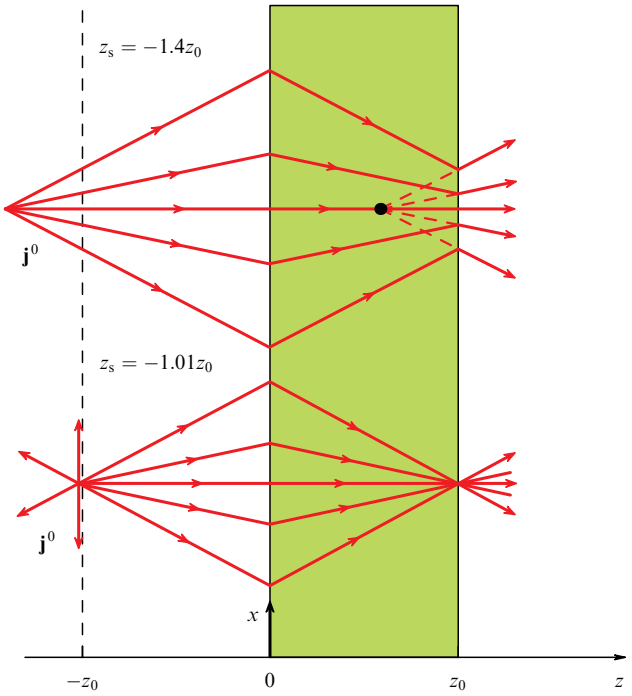

Figure 2. Energy flow lines for two positions of a point source removed from the lens by a distance exceeding its thickness; coordinates z_s of the source are indicated in the figure; point of convergence of dashed lines in the upper half of the figure indicates the position of the imaginary image of the source.

inside and behind the layer. In particular, if the field $\mathbf{E}^0$, $\mathbf{H}^0$ is induced by current (10), then, according to Eqns (5), the sources of the field $\mathbf{E}$, $\mathbf{H}$ are of the form

$$\mathbf{j} = \mathbf{j}^0 + \mathbf{j}^- + \mathbf{j}^+ ,$$

$$\mathbf{j}_\perp^- = -\mathbf{J}_\perp \delta(\mathbf{r}_\perp)\delta(z + z_s) , \quad j_z^- = J_z \delta(\mathbf{r}_\perp)\delta(z + z_s) , \qquad (11)$$

$$\mathbf{j}^+ = \mathbf{J}\delta(\mathbf{r}_\perp)\delta(z - z_s - 2z_0) .$$

As shown in Fig. 3, additional sources $\mathbf{j}^-$, $\mathbf{j}^+$ are located at the points where the images of source $\mathbf{j}^0$ should have been. Therefore, in the case under consideration, Eqns (4) and (6) describe not the image of source $\mathbf{j}^0$ but the radiation field of three extraneous sources that exchange energy with each other: the energy flows from sources $\mathbf{j}^0$ and $\mathbf{j}^+$ to source $\mathbf{j}^-$, which plays the role of an energy absorber (see the arrow directions in Fig. 3). A similar solution to the problem of the field formed by three sources of the indicated type in a space with a layer of the left-handed medium was previously obtained in a different way in Refs [38, 39].*

4. Model of an electromagnetic field forming an ideal image of a point source on the rear lens surface

When the source is located in the plane $z = z_s = -z_0$ and the rear surface of the lens ($z = z_0$) serves as the image plane, the expressions for the fields $\mathbf{E}$, $\mathbf{H}$ that form this image have a very simple form. Let us denote by $\hat{\mathbf{E}}(\mathbf{r}_\perp, z)$, $\hat{\mathbf{H}}(\mathbf{r}_\perp, z)$ the complex amplitudes of the EM field strengths of the dipole source

$$\hat{\mathbf{j}} = \mathbf{J}\delta(\mathbf{r}_\perp)\delta(z) \qquad (12)$$

* See also Ref. [42]. (*Author's note to English proof.*)

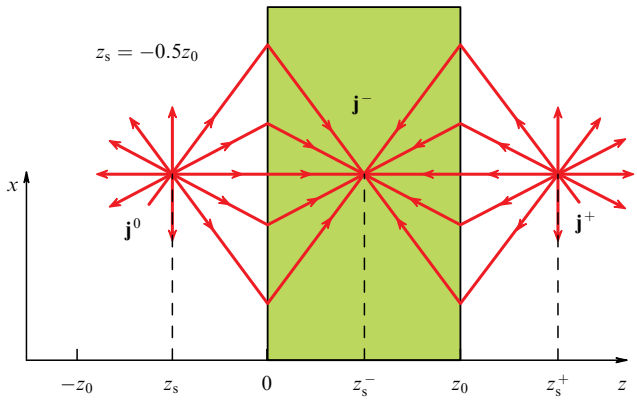

Figure 3. Energy flow lines in the presence of phantom sources $\mathbf{j}^-$ and $\mathbf{j}^+$; real source $\mathbf{j}^0$ is removed from the lens by a distance equal to half its thickness; z_s, z_s^-, and z_s^+ are the coordinates of the sources.

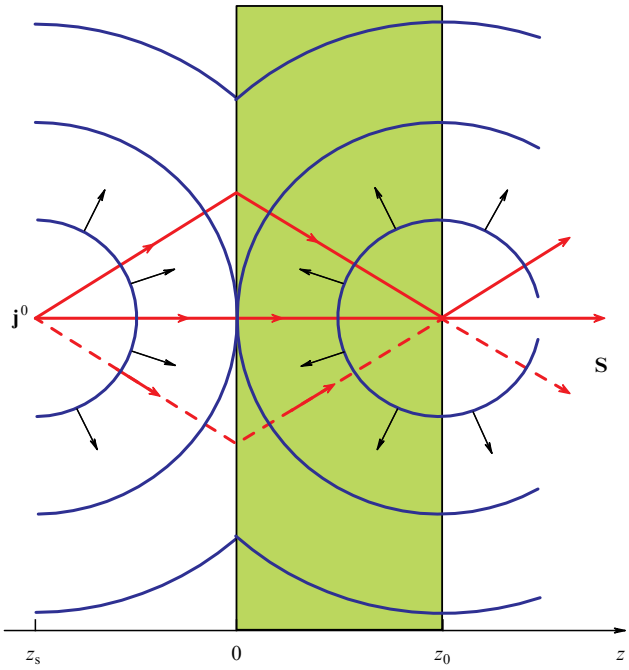

Figure 4. Formation of an ideal image of a point source under the condition $z_s = -z_0$; directions of propagation of phase fronts are shown by thin arrows, directions of the Umov–Poynting vector $\mathbf{S}$ are shown by thick arrows.

in free space. Then, according to Eqns (4), the electric field produced by the current (10) under the condition $z_s = -z_0$ is represented in terms of the function $\hat{\mathbf{E}}$ using the equations

$$\mathbf{E}(\mathbf{r}_\perp, z) = \hat{\mathbf{E}}(\mathbf{r}_\perp, z + z_0) \text{ for } -z_0 < z < 0 ,$$

$$\mathbf{E}_\perp(\mathbf{r}_\perp, z) = \hat{\mathbf{E}}_\perp(\mathbf{r}_\perp, z_0 - z) , \quad E_z(\mathbf{r}_\perp, z) = -\hat{E}_z(\mathbf{r}_\perp, z_0 - z) \text{ for } 0 \leqslant z \leqslant z_0 ,$$

$$\mathbf{E}(\mathbf{r}_\perp, z) = \hat{\mathbf{E}}(\mathbf{r}_\perp, z - z_0) \text{ for } z > z_0 . \qquad (13)$$

Similar formulas for calculating the magnetic field are obtained from expressions (13) by replacing $\mathbf{E} \to \mathbf{H}$, $\hat{\mathbf{E}} \to \hat{\mathbf{H}}$.

As shown in Fig. 4, when a spherical wave is incident on the front surface of the lens, a spherical wave is excited inside and behind it, with the phase center at the location point of the image of the source $\mathbf{r}_\perp = 0$, $z = z_0$ and with the phase

fronts propagating away from the phase center. Inside the lens, the Umov–Poynting vector is directed towards the phase center of this wave, and behind the lens it is directed away from the phase center. At the phase center, the field strength and energy flux density become infinity but do not experience a discontinuity that could lead to the emergence of a phantom source.

5. Elimination of phantom sources using the auxiliary-source method

We assume that the EM field $\mathbf{E}^0$, $\mathbf{H}^0$ incident on the lens is produced by sources located in the plane $z = z_s > -z_0$, for example, by electric current

$$\mathbf{j}^0 = \mathbf{J}(\mathbf{r}_\perp)\delta(z - z_s)\,. \tag{14}$$

The field $\mathbf{E}^0(\mathbf{r}_\perp, z)$ in the region of free space $z > z_s$ can be represented in terms of its distribution in the plane $z = 0$ in the form

$$\mathbf{E}^0(\mathbf{r}_\perp, z) = \iint \tilde{\mathbf{E}}(\mathbf{k}_\perp) \exp\left(-\mathrm{i}\mathbf{k}_\perp\mathbf{r}_\perp - \mathrm{i}k_z z\right) \mathrm{d}\mathbf{k}_\perp\,, \quad z_s < z < \infty\,, \tag{15}$$

$$k_z = \begin{cases} \sqrt{k_0^2 - k_\perp^2}\,, & k_\perp < k_0\,, \\ -\mathrm{i}\sqrt{k_\perp^2 - k_0^2}\,, & k_\perp > k_0\,, \end{cases} \tag{16}$$

$$\tilde{\mathbf{E}}(\mathbf{k}_\perp) = (2\pi)^{-2} \iint \mathbf{E}^0(\mathbf{r}_\perp, 0) \exp\left(\mathrm{i}\mathbf{k}_\perp\mathbf{r}_\perp\right) \mathrm{d}\mathbf{r}_\perp\,. \tag{17}$$

Note that the field $\mathbf{E}(\mathbf{r}_\perp, z)$ inside and behind the lens does not respond to changes in the source characteristics at which the field incident on the lens remains invariable. Therefore, the emergence of phantom sources could be prevented if it were possible to replace the real source (14) with an auxiliary source $\mathbf{j}^{\mathrm{aux}}$ located in the region $z < -z_0$ but creates the same field $\mathbf{E}^0(\mathbf{r}_\perp, 0)$ on the lens surface (plane $z = 0$), just like the real source. After performing this operation, the field $\mathbf{E}$ in the space with the lens could be expressed using the TO equations in terms of the field $\mathbf{E}^{\mathrm{aux}}(\mathbf{r}_\perp, z)$ produced by the auxiliary source in the free space region $z \geqslant -z_0$.

The $\mathbf{E}^{\mathrm{aux}}$ field must satisfy two requirements: it must coincide with the $\mathbf{E}^0$ field in the region $z_s < z < \infty$ and it must have no sources for $z \geqslant -z_0$. Therefore, it is natural to assume that the model of this field can be built by replacing the interval of variation of variable z in formula (15) with a broader interval $-z_0 \leqslant z < \infty$. The field found in this way will be expressed in terms of the spatial spectrum of the field $\tilde{\mathbf{E}}$ incident on the lens using an equation that differs from equation (15) only by the interval of variation of variable z:

$$\mathbf{E}^{\mathrm{aux}}(\mathbf{r}_\perp, z) = \iint \tilde{\mathbf{E}}(\mathbf{k}_\perp) \exp\left(-\mathrm{i}\mathbf{k}_\perp\mathbf{r}_\perp - \mathrm{i}k_z z\right) \mathrm{d}\mathbf{k}_\perp \quad \text{for} \quad -z_0 \leqslant z < \infty\,. \tag{18}$$

The field $\mathbf{E}$ is found using formulas (4), in which the function $\mathbf{E}^0$ is replaced by the function $\mathbf{E}^{\mathrm{aux}} = \mathbf{E}_\perp^{\mathrm{aux}} + E_z^{\mathrm{aux}}\mathbf{z}_0$:

$$\mathbf{E}_\perp(\mathbf{r}_\perp, z) = \mathbf{E}_\perp^{\mathrm{aux}}\left(\mathbf{r}_\perp, \xi(z)\right)\,, \qquad E_z(\mathbf{r}_\perp, z) = \frac{\mathrm{d}\xi(z)}{\mathrm{d}z}\, E_z^{\mathrm{aux}}\left(\mathbf{r}_\perp, \xi(z)\right) \text{ when } z_s < z < \infty\,. \tag{19}$$

After substituting function (7) into Eqns (19), they assume the form

$$\begin{aligned} &\mathbf{E}(\mathbf{r}_\perp, z) = \mathbf{E}^{\mathrm{aux}}(\mathbf{r}_\perp, z) = \mathbf{E}^0(\mathbf{r}_\perp, z) \text{ for } z_s < z < 0\,, \\ &\mathbf{E}_\perp(\mathbf{r}_\perp, z) = \mathbf{E}_\perp^{\mathrm{aux}}(\mathbf{r}_\perp, -z)\,, \quad E_z(\mathbf{r}_\perp, z) = -E_z^{\mathrm{aux}}(\mathbf{r}_\perp, -z) \\ &\text{for } 0 \leqslant z \leqslant z_0\,, \\ &\mathbf{E}(\mathbf{r}_\perp, z) = \mathbf{E}^{\mathrm{aux}}(\mathbf{r}_\perp, z - 2z_0) \text{ for } z > z_0\,. \end{aligned} \tag{20}$$

The expressions for the magnetic field are obtained by replacing $\mathbf{E} \to \mathbf{H}$, $\mathbf{E}^0 \to \mathbf{H}^0$, $\tilde{\mathbf{E}} \to \tilde{\mathbf{H}}$, $\mathbf{E}^{\mathrm{aux}} \to \mathbf{H}^{\mathrm{aux}}$ in formulas (15)–(20).

We illustrate the outlined method of eliminating phantom sources with two simple examples.

(1) As a source, we consider a sinusoidally nonuniform electric current

$$\mathbf{j}^0 = I\mathbf{y}_0 \cos\left(k_y y\right) \delta(z - z_s) \tag{21}$$

with spatial frequency $k_y > k_0$, at which the EM field becomes reactive:

$$\begin{aligned} &\mathbf{H}^0 = H_x^0 \mathbf{x}_0\,, \\ &H_x^0(y, z) = A \operatorname{sgn}(z - z_s) \cos\left(k_y y\right) \exp\left(-\alpha|z - z_s|\right)\,, \\ &A = \frac{2\pi I}{c}\,, \quad \alpha = \sqrt{k_y^2 - k_0^2}\,, \quad \mathbf{E}^0 = -\mathrm{i}k_0^{-1} \operatorname{rot} \mathbf{H}^0\,, \quad z \neq z_s\,. \end{aligned} \tag{22}$$

Using the auxiliary field

$$H_x^{\mathrm{aux}}(y, z) = A \cos\left(k_y y\right) \exp\left[-\alpha(z - z_s)\right] \tag{23}$$

and formulas like Eqns (20), we find the magnetic field in the space with the lens:

$$H_x = A \cos\left(k_y y\right) \begin{cases} \exp\left[\alpha(z_s - z)\right]\,, & z_s < z < 0\,, \\ \exp\left[\alpha(z + z_s)\right]\,, & 0 < z < z_0\,, \\ \exp\left[\alpha(z_s + 2z_0 - z)\right]\,, & z_0 < z < \infty\,. \end{cases} \tag{24}$$

As shown in Fig. 5, the resultant dependence of the field strength on the z coordinate is not distorted by phantom sources and correctly describes the effect of reactive field enhancement inside the lens.

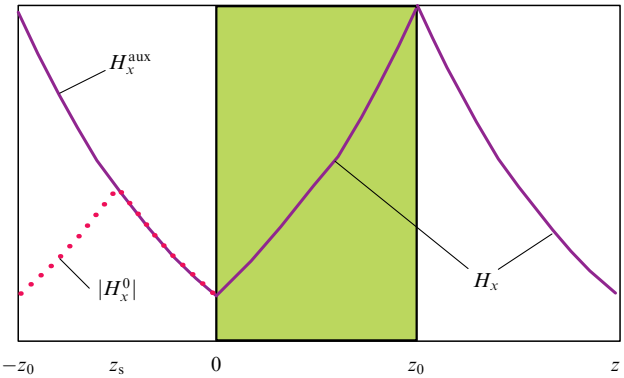

Figure 5. Illustration of the effect of amplification of the reactive EM field in the layer of the 'left-handed' medium $0 < z < z_0$. Dotted curve shows the modulus of the function $H_x^0(0, z)$ for $z < 0$, and the solid curve shows the function $H_x^{\mathrm{aux}}(0, z)$ for $z < 0$ and the function $H_x(0, z)$ for $z > z_s$.

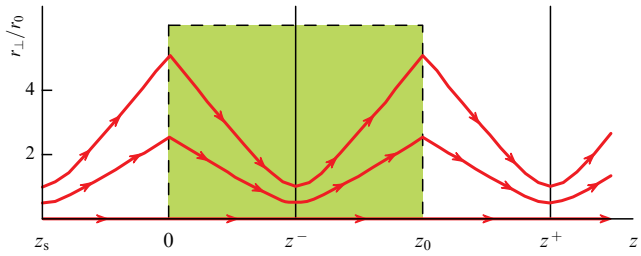

Figure 6. Lines of the energy flow passing through the lens under the conditions $z_s = -z_0/2$, $k_0 r_0^2/z_0 = 0.1$; z^- and z^+ are planes of the source images.

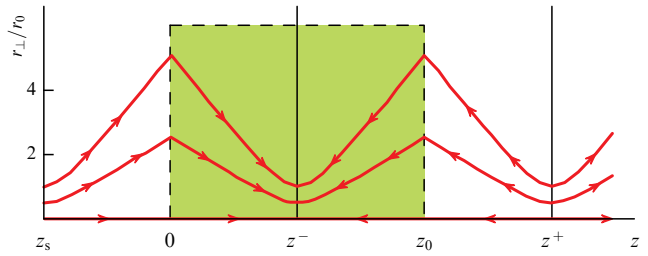

Figure 7. Lines of energy flow through the lens calculated without the operation of eliminating phantom sources; for $z^- < z < z^+$, energy flows in Figs 6 and 7 are directed in opposite directions.

(2) Let us assume that the lens is irradiated by a wave beam produced by a source of the form

$$\mathbf{j}^0 = I\mathbf{y}_0 \exp\left(-\frac{r_\perp^2}{2r_0^2}\right)\delta(z - z_s)\,, \quad k_0 r_0 \gg 1\,. \tag{25}$$

In the quasi-optical approximation, the field of this source is described by the formulas

$$E_y^0(r_\perp, z) = \frac{A}{f(z)} \exp\left[-\mathrm{i}k_0\big(|z - z_s|\big) - \frac{r_\perp^2}{2r_0^2 f(z)}\right], \qquad H_x^0 = E_y^0 \operatorname{sgn}(z - z_s)\,, \quad f(z) = 1 - \mathrm{i}\,\frac{|z - z_s|}{k_0 r_0^2}\,. \tag{26}$$

The expression for the auxiliary-source field $E_y^{\mathrm{aux}}(r_\perp, z)$ is obtained from formulas (26) by replacing $|z - z_s| \to (z - z_s)$, after which we take advantage of Eqns (20) to find the field distribution in and behind the lens.

Figure 6 shows the calculated energy flow lines in the EM field which forms images of the source (25) inside and behind the lens. The components of the Umov–Poynting vector for the auxiliary $(\mathbf{E}^{\mathrm{aux}}, \mathbf{H}^{\mathrm{aux}})$ and real $(\mathbf{E}, \mathbf{H})$ fields were represented as

$$S_z^{\mathrm{aux}}(r_\perp, z) = \frac{S_z^{\mathrm{aux}}(0,0)}{g(z)} \exp\left[-\frac{r_\perp^2}{r_0^2 g(z)}\right], \quad g(z) = 1 + \frac{(z - z_s)^2}{k_0^2 r_0^4}\,, \tag{27}$$

$$S_\perp^{\mathrm{aux}}(r_\perp, z) = \frac{r_\perp S_z^{\mathrm{aux}}(0,0)}{2g^2(z)} \frac{\mathrm{d}g(z)}{\mathrm{d}z} \exp\left[-\frac{r_\perp^2}{r_0^2 g(z)}\right], \quad z > -z_0\,, \tag{28}$$

$$S_z(r_\perp, z) = S_z^{\mathrm{aux}}\big(r_\perp, \xi(z)\big)\,, \tag{29}$$

$$S_\perp(r_\perp, z) = \frac{\mathrm{d}\xi(z)}{\mathrm{d}z}\, S_\perp^{\mathrm{aux}}\big(r_\perp, \xi(z)\big)\,, \quad z > z_s\,.$$

The following equation was used to construct energy flow lines:

$$\frac{\mathrm{d}r_\perp}{\mathrm{d}z} = \frac{S_\perp\big(r_\perp, \xi(z)\big)}{S_z\big(r_\perp, \xi(z)\big)}\,, \tag{30}$$

whose solution is of the form

$$\frac{r_\perp(z)}{r_\perp(z_s)} = \sqrt{g\big(\xi(z)\big)} = \sqrt{1 + k_0^{-2} r_0^{-4} \big(\xi(z) - z_s\big)^2}\,. \tag{31}$$

Shown for comparison in Fig. 7 are the energy flow lines constructed according to formulas (6), (7) without replacing the real source with an auxiliary one. As one can see from Fig. 7, in this case, the z-component of the energy flux density in the source image planes $z = \{z^-, z^+\}$ changes sign, which indicates the presence of phantom sources in these planes.

Note that the operation of replacing fields $\mathbf{E}^0, \mathbf{H}^0 \to \mathbf{E}^{\mathrm{aux}}, \mathbf{H}^{\mathrm{aux}}$ in formulas (4) can be considered in the replacing the EM field of the observed radiation source to be region $-z_0 < z < 0$ with a field that produces an ideal image of this source. After such a replacement, the object of observation for the lens is not the radiation source but the already prepared image of this source, which the lens merely copies. In this case, phantom sources do not emerge, because there is no source in the EM field being copied.

This brings up the natural question: is the auxiliary-source method suitable for eliminating phantom sources in the theoretical image model of a dipole source (10) with coordinate $z_s > -z_0$? To provide the answer, let's turn to Fig. 8, which shows the patterns of energy flows in free space for the source $\mathbf{j}^0 = I\mathbf{y}_0 \delta(\mathbf{r}_\perp)\delta(z - z_s)$ and the auxiliary source that produces the EM field $\mathbf{E}^{\mathrm{aux}}, \mathbf{H}^{\mathrm{aux}}$.

According to Fig. 8, the field of the auxiliary source in the region $-z_0 < z < z_s$ is an EM wave, which focuses at the point $\mathbf{r}_\perp = 0$ of the plane $z = z_s$ and, after passing through this plane, turns into a copy of the field of a point source (in accordance with the statement about the field of the auxiliary source forming an ideal image of the real source). The problem is that, in the auxiliary field, the energy fluxes along the 'illuminated' and 'shadow' sides of the plane $z = z_s$ at $\mathbf{r}_\perp \neq 0$ are oppositely directed (Fig. 8b) and, therefore, the continuity condition for this field is not satisfied. Thus, a model of an ideal image of a dipole source located in the region $-z_0 < z < 0$ cannot be built, since Maxwell's equations do not allow the possibility of its existence.

As shown above, this problem does not arise when calculating images of the sources of reactive fields and wave beam type fields. Apparently, the continuity of the auxiliary

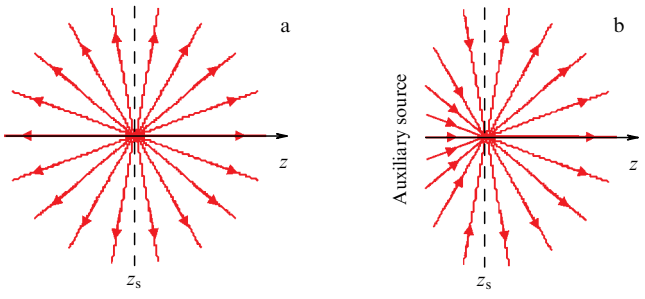

Figure 8. Lines of energy flow in the plane $y = 0$ from (a) a point source and (b) an auxiliary source, constructed on the basis of a qualitative analysis of formulas (15)–(18).

field will not be violated either when the spatial spectrum of the field incident on the lens satisfies the condition $\tilde{\mathbf{E}}(\mathbf{k}_\perp) \to 0$ as $k_\perp \to k_0$.

Interestingly, when a point source is located in the plane $z = -z_0$ (see Fig. 4), the energy fluxes along the inner and outer sides of the rear lens surface are also oppositely directed. However, this does not violate the continuity of the field, since the wave propagates inside the lens in the direction opposite to the **S** vector.

6. Conclusions

To explain the mechanism of image formation by a Veselago lens, a pattern is often used depicting rays that emerge from a radiation source at different angles and, after refraction at the boundaries of the layer of a 'left-handed' medium, intersect first inside the layer and then behind it to produce two images of the source. Meanwhile, in a spatially coherent monochromatic EM field, rays (energy flow lines) intersect (or, more precisely, originate or terminate) only at the location points of the sources and sinks of energy. And in the plane of the image of the source, they approach as close as possible, and then diverge without intersecting. Therefore, the picture of intersecting rays described above should be considered an illustration of the EM field model of three external sources, two of which are phantom. This model cannot be used to analyze the resolving power of the Veselago lens, but, nevertheless, it turns out to be in demand: one of the ideas for implementing atom excitation in the scheme of a quantum computer relies on it [40, 41].

The TO equations given in this paper can be conveniently used to demonstrate the ability of the Veselago lens to copy the EM fields of sources that are outside its field of view. They make it possible to construct a very simple model of the image of an arbitrary point source located at a distance from the lens equal to its thickness. They can also be used to study the image of a closely located source, provided that it can be replaced by a distant source without changing the characteristics of the field incident on the lens.

When the distance between the source and the lens exceeds its thickness, it produces an imaginary image of the source shifted relative to the source towards the lens by twice its thickness. A real ideal image of an arbitrary point source is produced by an ideal Veselago lens only when the image is located on the rear surface of the lens.[1] This can be explained by the fact that only in this case are conditions laid for the production of the correct ray pattern of the image due to the refraction of rays on the lens surfaces: the front surface collects all the rays at one point on the rear surface, and the rear surface makes the collected rays diverge, preventing them from intersecting. If the source is at a shorter distance from the lens than its thickness, then a model of its image can be developed only if certain requirements for the source characteristics are met. An ideal image model of a dipole source with coordinate $z_s > -z_0$ cannot be constructed, because Maxwell's equations do not allow it.[2]

In conclusion, we note that, in order to verify the correctness of EM field calculations in lenses with losses, it is necessary to ensure that no phantom sources emerge when losses tend to zero.

[1] The optimality of such a configuration in the presence of losses in the lens was proved in Ref. [12].

[2] The authors of Refs [19, 20] arrive at a similar conclusion for some other reasons.

Acknowledgements. This work was carried out in the framework of State Assignment FFUF-2021-0006.

References

1. Veselago V G *Sov. Phys. Usp.* **10** 509 (1968); *Usp. Fiz. Nauk* **92** 517 (1967)
2. Veselago V G *Sov. Phys. Solid State* **8** 2853 (1967); *Fiz. Tverd. Tela* **8** 3571 (1966)
3. Pendry J B *Phys. Rev. Lett.* **85** 3966 (2000)
4. Shelby R A, Smith D R, Schultz S *Science* **292** 77 (2001)
5. Cummer S A *Appl. Phys. Lett.* **82** 1503 (2003)
6. Rao X S, Ong C K *Phys. Rev. B* **68** 113103 (2003)
7. Lagarkov A N, Kissel V N *Phys. Rev. Lett.* **92** 077401 (2004)
8. Pendry J B *Contemp. Phys.* **45** (3) 191 (2004)
9. Grbic A, Eleftheriades G V *Phys. Rev. Lett.* **92** 117403 (2004)
10. Smith D R, Pendry J B, Wiltshire M C K *Science* **305** 788 (2004)
11. Merlin R *Appl. Phys. Lett.* **84** 1290 (2004)
12. Podolskiy V A, Kuhta N A, Milton G W *Appl. Phys. Lett.* **87** 231113 (2005)
13. Fang N et al. *Science* **308** 534 (2005)
14. Lee H et al. *New J. Phys.* **7** 255 (2005)
15. Melville D O S, Blaikie R J *Opt. Express* **13** 2127 (2005)
16. Podolskiy V A, Narimanov E E *Opt. Lett.* **30** (1) 75 (2005)
17. Veselago V G et al. *J. Comput. Theor. Nanosci.* **3** 189 (2006)
18. Lagarkov A N et al. *Phys. Usp.* **52** 959 (2009); *Usp. Fiz. Nauk* **179** 1018 (2009)
19. Collin R E *Prog. Electromagn. Res. B* **19** 233 (2010)
20. Gralak B, Maystre D *C.R. Phys.* **13** 786 (2012)
21. Lagarkov A N, Kisel V N *Energiya: Ekonomika, Tekh., Ekologiya* (1) 10 (2018)
22. Selina N V *Phys. Usp.* **65** 406 (2022); *Usp. Fiz. Nauk* **192** 443 (2022)
23. Nicorovici N A, McPhedran R C, Milton G W *Phys. Rev. B* **49** 8479 (1994)
24. Smith D R et al. *Appl. Phys. Lett.* **82** 1506 (2001)
25. Pendry J B *Opt. Express* **11** 755 (2003)
26. Milton G et al. *Proc. R. Soc. A* **461** 3999 (2005)
27. Yan M, Yan W, Qiu M *Phys. Rev. B* **78** 125113 (2008)
28. Ammari H et al. *Proc. R. Soc. A* **469** 20130048 (2013)
29. McPhedran R C, Milton G W *C.R. Phys.* **21** 409 (2020)
30. Dolin L S *Radiophys. Quantum Electron.* **64** 126 (2021); *Izv. Vyssh. Uchebn. Zaved. Radiofiz.* **64** (2) 138 (2021)
31. Dolin L S *J. Opt. Soc. Am. B* **38** 2338 (2021)
32. Pendry J B, Schurig D, Smith D R *Science* **312** 1780 (2006)
33. Dolin L S *Izv. Vyssh. Uchebn. Zaved. Radiofiz.* **4** 964 (1961)
34. Post E J *Formal Structure of Electromagnetics: General Covariance and Electromagnetics* (New York: Interscience Publ., 1962)
35. Lax M, Nelson D F *Phys. Rev. B* **13** 1777 (1976)
36. Ward A J, Pendry J B *J. Mod. Opt.* **43** 773 (1996)
37. Leonhardt U, Philbin T G *New J. Phys.* **8** 247 (2006)
38. Guzatov D V, Klimov V V *Quantum Electron.* **44** 873 (2014); *Kvantovaya Elektron.* **44** 873 (2014)
39. Guzatov D V, Klimov V V *Quantum Electron.* **44** 1112 (2014); *Kvantovaya Elektron.* **44** 1112 (2014)
40. Klimov V V *Phys. Usp.* **64** 990 (2021); *Usp. Fiz. Nauk* **191** 1044 (2021)
41. Klimov V V *Phys. Usp.* **66** 263 (2023); *Usp. Fiz. Nauk* **193** 279 (2023)
42. Klimov V V *JETP Lett.* **89** 229 (2009); *Pis'ma Zh. Eksp. Teor. Fiz.* **89** 270 (2009)